Role of NO_3 in sulfate production in the wintertime northern latitudes

Graham Feingold
NOAA Environmental Technology Laboratory, Boulder, Colorado, USA

Gregory J. Frost[1] and A. R. Ravishankara[2]
NOAA Aeronomy Laboratory, Boulder, Colorado, USA

Received 12 March 2002; revised 22 July 2002; accepted 25 July 2002; published 22 November 2002.

[1] The production of sulfate via multiphase chemistry is usually assumed to be dominated by oxidation of S(IV) by O_3 and H_2O_2. The former reaction is *p*H dependent and negligibly small for *p*H less than about 5, while oxidation via H_2O_2 is independent of *p*H. Another oxidant that may play a role in sulfate formation is NO_3 [*Sander et al.*, 1995; *Mozurkewich*, 1995; *Rudich et al.*, 1998]. Although it is commonly assumed to be far less important than O_3 and H_2O_2, it has been hypothesized that it may account for significant oxidation under certain conditions, such as relatively low mixing ratios of O_3 and <150 pptv of H_2O_2. These conditions may be met in the nighttime Northern Hemisphere winters when H_2O_2 production is small and NO_x concentrations are sufficient to produce adequate concentrations of NO_3. We explore the importance of NO_3 in multiphase sulfate production using a simple cloud model. It is shown that the relative importance of NO_3 is very sensitive to the assumed value of the Henry's Law equilibrium constant of NO_3 as well as the assumed catalytic chain length for NO_3 oxidation of S(IV). Using the recently measured value of 0.6 M atm^{-1} [*Rudich et al.*, 1996], and a catalytic chain length of 8, it is shown that NO_3 enhances sulfate production by about 10–30% relative to calculations where NO_3 is absent. It is noted that NO_3 may contribute even more if additional sources of NO_x are present and/or H_2O_2 is removed via precipitation. *INDEX TERMS:* 0305 Atmospheric Composition and Structure: Aerosols and particles (0345, 4801); 0320 Atmospheric Composition and Structure: Cloud physics and chemistry; 0322 Atmospheric Composition and Structure: Constituent sources and sinks; 0345 Atmospheric Composition and Structure: Pollution—urban and regional (0305); *KEYWORDS:* clouds, multiphase chemistry, nitrogen oxides, sulfate

Citation: Feingold, G., G. J. Frost, and A. R. Ravishankara, Role of NO_3 in sulfate production in the wintertime northern latitudes, *J. Geophys. Res.*, *107*(D22), 4640, doi:10.1029/2002JD002288, 2002.

1. Introduction

[2] Oxidation of sulfur dioxide, SO_2, to sulfuric acid or sulfate (H_2SO_4 or SO_4^{2-}) in the troposphere is a key process that leads to sulfate aerosol and acid precipitation. The role of sulfate aerosols in climate forcing has been the focus of much attention because it can offset greenhouse gas forcing; there is, however, considerable uncertainty in the magnitude of this aerosol forcing. The production of acid rain has been a continuing issue over the past several decades and there have been many policy decisions taken to curb it. Currently, it is believed that the vast majority of SO_2 is oxidized in the troposphere in the gas phase via its reaction with OH or in the condensed phase via its reactions with H_2O_2 and O_3. The oxidants OH, H_2O_2, and O_3 are photochemically produced in the gas phase. The OH radical is very short-lived and its abundance is essentially zero in the dark. The more stable H_2O_2, which is produced in the gas phase via the reactions of HO_2 with itself, is maximized during daytime and decays in the dark due to multiphase reactions, scavenging, and surface deposition. The longer-lived ozone is also photochemically produced but, generally, it is less efficient at oxidizing SO_2 in the liquid phase than H_2O_2. Therefore, the majority of SO_2 is believed to be oxidized during daylight hours and restricted to regions that experience significant photochemistry.

[3] A few modeling studies of global sulfate production have been carried out [*Kasibhatla et al.,* 1997; *Barth et al.* 2000]. These investigations underpredict the extent of sulfate formation in the northern high latitudes, especially during periods when there is less sunlight as in wintertime. There may be many reasons for this underprediction but bearing in mind that a large fraction of sulfate is produced in clouds, and that the average cloud cover in the winter months at these locations is about 80% [*Warren et al.*, 1986a, 1986b], a multiphase source is not unreasonable. In this paper, we explore the possible contribution of the nitrate

[1]Also at Cooperative Institute for Research in the Environmental Sciences, University of Colorado, Boulder, Colorado, USA.
[2]Also at Department of Chemistry and Biochemistry, University of Colorado, Boulder, Colorado, USA.

Copyright 2002 by the American Geophysical Union.
0148-0227/02/2002JD002288$09.00

Table 1. Input to the Gas-Phase Model

Parameter	Value
date	Dec. 21
latitude	50°N
pressure	1000 mbar
temperature	5°C
relative humidity	70%
H_2O mixing ratio	3.8 g kg^{-1}
$[NO_x]$	1 ppbv
$[O_3]$	40 ppbv
[ethene]	2 ppbv
[propene]	80 pptv
aerosol surface area	10^{-7} cm^2/cm^3
$\gamma(N_2O_5)$	0.05
$\gamma(NO_3)$	2×10^{-4}

radical, NO_3, as an oxidant of SO_2. The nitrate radical is essentially a "nighttime" radical because of its rapid photolysis during daytime. Therefore, it is reasonable to expect a significant role for NO_3 in the wintertime at high latitudes. Furthermore, the majority of the northern SO_2 is anthropogenic in origin and is mostly due to fossil fuel burning, which also generates nitrogen oxides. These nitrogen oxides can be the source of NO_3. Some previous investigations have suggested a role for NO_3 in oxidizing SO_2 [*Mozurkewich*, 1995; *Sander et al.*, 1995; *Rudich et al.*, 1998]. Many of the parameters needed to estimate the rate of oxidation of SO_2 by NO_3 are known, but there are some uncertainties in their values. Box model studies [*Mozurkewich*, 1995; *Sander et al.*, 1995] have shown that SO_2 oxidation can be efficient in droplets due to the catalytic nature of the SO_2 oxidation initiated by a free radical, such as NO_3, in water.

[4] In this paper, we explore SO_2 oxidation by NO_3 under conditions where the abundances of OH and H_2O_2 are limited. We assume that OH is absent because it is dark, and that the abundance of H_2O_2 is derived from its daytime production. These conditions are not representative of all high latitudes but may be considered typical of northern Europe during winter.

2. Models

[5] A simple modeling approach is adopted to assess some bounds on the effect of NO_3. As a first step, a photochemical box model is used to simulate the pertinent high-latitude, northern hemisphere gas-phase chemistry and a self-consistent set of gas phase constituents. Then, the output from the gas-phase model is used as input to a multiphase chemical model, which is run for nighttime conditions for a period of 8 h. There is no feedback of one model to the other but this is reasonable since in the absence of photochemistry, the primary change to the gaseous components is through uptake on droplets and multiphase chemistry. Even though the separation is artificial, it represents a good first step to investigate the effect of multiphase NO_3 chemistry on SO_2 oxidation. Future work should run the two models interactively. The two models are described below.

2.1. Photochemical Box Model

[6] The photochemical box model is very similar to that described by *Frost et al.* [1998]. Thermal rate coefficients are taken from *DeMore et al.* [1997] and, when not available there, from *Atkinson* [1994]. Photolysis rate coefficients are calculated off-line using a radiative transfer model (S. J. Madronich, J. Zeng, and K. Stamnes, TUV: Tropospheric ultraviolet-visible radiation model, Version 3.8, http://www.acd.ucar.edu/TUV/, 1997). $[N_2]$, $[O_2]$, $[H_2O]$, $[CH_4]$, temperature, and pressure are held constant in this model calculation, while all other chemical species are allowed to vary with time. Input conditions for selected variables are listed in Table 1. These conditions are representative of a pollution plume approximately 1 day downwind of the source, in that $[NO_x]$ and $[SO_2]$ concentrations have decreased (through dilution and reaction) from those that would be observed in fresh emissions. Because the plume is chemically "aged," the chemistry of the more reactive nonmethane hydrocarbons can be ignored. During the night and away from sources, [NO] is assumed to be 0, so that $[NO_x] = [NO] + [NO_2] = [NO_2]$. The model chemistry that controls $NO_3(g)$ levels is summarized in Table 2. The model includes two heterogeneous chemical reactions, namely the uptake of $N_2O_5(g)$ and $NO_3(g)$ on background hydrated aerosol (reactions (R5) and (R6)). The reactive uptake coefficients, γ, for reactions (R5) and (R6) [*DeMore et al.*, 1997] and the aerosol surface area used are given in Table 1.

2.2. Multiphase Model

[7] Multiphase sulfate production is simulated using a cloud parcel model coupled to a simple multiphase chemistry model [*Feingold et al.*, 1998; *Zhang et al.*, 1999]. In the latter studies, sulfate oxidation was due to O_3 and H_2O_2, using rate constants given by *Hoffmann and Calvert* [1985]. Here the mechanism is extended to simulate oxidation via NO_3. For a prescribed rate of ascent, the cloud model calculates the uptake of water vapor by a size distribution of ammonium sulfate aerosol particles, the formation of droplets, and their growth by condensation. Using a time-splitting technique at an interval of 1 s, the model simulates the dissolution of soluble gases into the droplets, and the conversion of S(IV) to S(VI). The time-splitting between microphysics and multiphase chemistry has been shown to

Table 2. Nighttime Model Chemistry of NO_3 and N_2O_5[a]

Reaction	Reaction
(R1)	$NO_2 + O_3 \rightarrow NO_3 + O_2$
(R2a)	$NO_3 + NO_2 + M \rightarrow N_2O_5 + M$
(R2b)	$N_2O_5 + M \rightarrow NO_3 + NO_2 + M$
(R3)	$N_2O_5 + H_2O \rightarrow 2HNO_3$
(R4)	$NO_3 + \text{ethene, propene} \rightarrow HNO_3 + \text{products}$
(R5)	$N_2O_5 + \text{hydrated aerosol} \rightarrow HNO_3 + \text{products}$
(R6)	$NO_3 + \text{hydrated aerosol} \rightarrow \text{products}$

[a] All reactions are in the gas phase.

be accurate provided the time-splitting interval is less than about 10 s [*Müller*, 2000].

[8] As initial conditions, the particle sizes are given at 10 logarithmically separated discrete sizes and the distribution is assumed to be lognormal, with a median radius of 0.06 μm, geometric standard deviation of 1.6, and total concentration of 500 cm^{-3}. These size distribution parameters are appropriate for moderately polluted conditions. The model uses predetermined kinematic trajectories as a source of thermodynamic properties. These are derived from a large eddy simulation (LES) of a stratocumulus-capped boundary layer cloud [*Stevens et al.,* 1996]. The advantage of this approach is that air parcels are constantly cycled in and out of cloud in a manner that is more representative of true boundary layer motions, rather than simply assuming that a parcel rises adiabatically, or has constant cloud liquid water (LWC) for an arbitrarily determined period of time. In general, the time that a parcel spends in contact with the cloud will depend on the extent of cloud cover and the degree to which the surface layer is coupled to the cloud layer; the simple scenario used here is not representative of all boundary layers (see section 3). The LES-derived parcels have a cloud contact time of about 10 minutes in every hour. Cloud contact is assumed to occur at night. The LWC varies along the parcel trajectory and has a maximum value of 0.28 g m^{-3}. The concentration of haze particles/droplets with radius >1 μm is ~270 cm^{-3}, i.e., only about half of the total number of aerosol particles grows to droplet sizes. The mean drop radius varies between ~1.5 μm near cloud base to ~6.5 μm at cloud top. Multiphase reactions occur whenever the haze particles/droplets are deemed to be sufficiently dilute (in our case, a concentration of <2 M).

[9] A Lagrangian technique is used to calculate the growth of droplets. An ordinary differential equation solver [*Brown et al.*, 1989] is used to solve coupled differential equations describing changes in particle/droplet radius in each of the 10 size categories. An additional set of differential equations describes diffusion-limited uptake of SO_2, O_3, H_2O_2, NH_3, HNO_3, CO_2, and NO_3 following *Pandis and Seinfeld* [1989]:

$$\frac{dC_i(g)}{dt} = -k_{mt,j}x_{l,j}C_i(g) + k_{mt,j}\frac{C_{i,j}(aq)}{K_H RT} + R_{i,j} \qquad (1)$$

$$\frac{dC_{i,j}(aq)}{dt} = k_{mt,j}x_{l,j}C_i(g) - k_{mt,j}\frac{C_{i,j}(aq)}{K_H RT} + R_{i,j}, \qquad (2)$$

where $R_{i,j}$ is the net rate of production of species i by chemical reactions in drop size class j, $k_{mt,j} = 3\eta_j D/r_j^2$ [*Pandis and Seinfeld*, 1989] is a combined rate coefficient for gas phase plus interfacial mass transport), r_j is the cloud droplet radius (cm), K_H is the effective Henry's law constant (mol L^{-1} atm^{-1}), R is the ideal gas constant (0.08206 L atm mol^{-1} K^{-1}), T is temperature (in Kelvin), and D is diffusivity in air (cm^2 s^{-1}). The coefficient η_j is related to the accommodation coefficient α and corrects for free molecular effects as approximated by *Fuchs and Sutugin* [1971], and $x_{l,j}$ is the liquid-water mixing ratio (L water/L air) in drop size class j. Values for the diffusion constant D are not known for all gases but a value of 0.1 cm^2 s^{-1} is assumed to be representative for most species [*Schwartz*, 1986]. The accommodation coefficients, α, are from *DeMore et al.* [1997], *Gardner et al.* [1987], and *Tang and Lee* [1987]. Drops are assumed to be well mixed but this assumption is expected to be of secondary importance, considering the other uncertainties.

[10] Although the gas and multiphase models are separate entities, a simple set of gas phase reactions must be solved during the course of the nighttime multiphase simulation in order to calculate NO_3 (g) and N_2O_5 (g). We assume a fixed [NO_2 (g)] and solve:

(R1) $$NO_2(g) + O_3(g) \rightarrow NO_3(g) + O_2(g)$$

(R2a) $$NO_3(g) + NO_2(g) + M \rightarrow N_2O_5(g) + M$$

(R2b) $$N_2O_5(g) + M \rightarrow NO_3(g) + NO_2(g) + M.$$

O_3 (g) is not fixed because it participates in multiphase chemistry; however it is not very soluble and therefore deviates little from its initial condition (Table 1). Gas concentrations of SO_2, O_3, H_2O_2, NH_3, and CO_2 have no sources and, if consumed, are not replenished. This is justified by our assumption that SO_2 and NH_3 are considered to have their source in the original plume emission and are not produced downwind of the emission. (HNO_3 is also assumed to derive from the plume but does have other sources, as will be discussed below.) Some H_2O_2 may be produced by reaction between HO_2 and HO_2 in the early evening but this is probably small. Variations in CO_2 are typically negligible.

[11] It is assumed that N_2O_5 is immediately converted to HNO_3 once in solution [*Lelieveld and Crutzen*, 1991], which constitutes a source of HNO_3. The fact that N_2O_5 is the acid anhydride of HNO_3 and thus not expected to remain intact upon contact with water precludes use of Equations 1 and 2 to describe uptake and outgassing. Therefore in contrast to the other gases, uptake of N_2O_5 onto drops is not treated as a diffusion-limited process but is parameterized based on the drop size distribution surface area. When drops evaporate, HNO_3 is returned to the ambient air. In general we do not consider permanent removal of HNO_3 as particulate inorganic nitrate. Sensitivity to this assumption is examined in section 4.2.3. Finally, to simplify the multiphase chain reactions for NO_3 it is assumed that 8 moles of S(VI) are produced for every mole of NO_3 consumed in solution [*Rudich et al.*, 1998]. Simulations are also performed to check the sensitivity of the results to the assumed chain length of the catalytic reaction (section 4.2.1).

3. Results

[12] The gas phase model is run for a period of 48 h (Figure 1) using input appropriate for the Northern Hemisphere winter (Table 1). Model output for O_3, NO, NO_2, NO_3 and N_2O_5 is shown in Figure 1. [NO_2] declines steadily over the course of the simulation while [NO_3] remains approximately constant. Most of the [NO_2] decline occurs at night through the loss of N_2O_5 by reactions (R3) and (R5) (Table 2); daytime production of NO_2 via the oxidation of NO by O_3 and HO_2 ceases at night because [NO] and [HO_2] rapidly become negligible after sunset. [NO_3] is relatively constant because it is buffered by simultaneous production by the reaction of NO_2 + O_3 (reaction (R1)), and from the thermal decomposition of N_2O_5 (reaction (R2b)). Results are not dependent on the

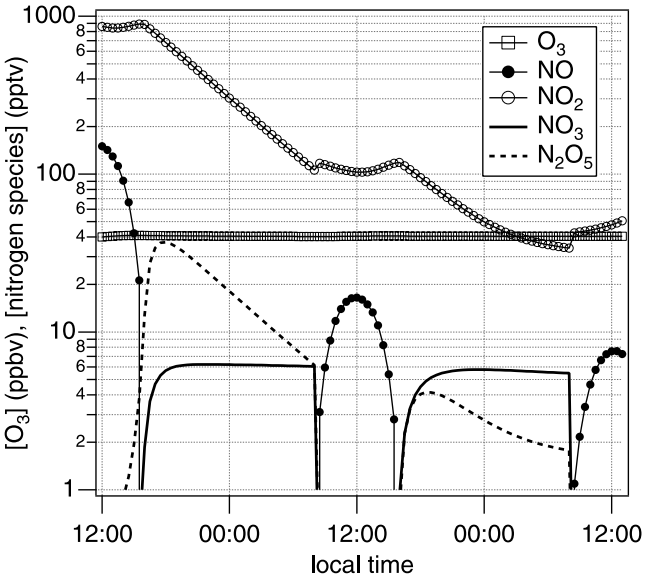

Figure 1. Gas phase model chemistry in the absence of clouds for input conditions in Table 1.

input H_2O_2; for example, the levels of O_3, NO, NO_2, NO_3 and N_2O_5 levels are essentially the same whether the initial $[H_2O_2]$ is 30 or 300 pptv. This effect is expected since H_2O_2 does not react directly with NO_3 and N_2O_5 in the gas phase, nor does it react with any of their nighttime sources.

[13] Figure 1 is used to derive initial conditions for the multiphase model. Two sets of initial gas phase conditions are used (Table 3). In both cases we use $[SO_2]$ = 1000 pptv, $[O_3]$ = 40 ppbv, $[NH_3]$ = 100 pptv, $[HNO_3]$ = 1000pptv and $[CO_2]$ = 360 ppmv. To investigate the relative importance of oxidation via $[H_2O_2]$ and $[NO_3]$, $[H_2O_2]$ is varied between 30 pptv and 300 pptv. Self-consistent sets of $[NO_2]$, $[NO_3]$ and $[N_2O_5]$ are taken from Figure 1 and are listed in Table 3.

[14] An air parcel is assumed to cycle through a nocturnal stratiform cloud, spending approximately 10 minutes of every hour in contact with cloud [*Feingold et al.,* 1998]; multiphase chemistry is therefore intermittent. The total simulation time is 8 hours. The degree of contact with cloud is in general dependent on the dynamical nature of the atmosphere. Under stable conditions likely to be encountered in winter, some air parcels will likely never enter cloud while those that originate in cloud may spend hours in cloud. The cloud exposure of 10 minutes per hour (~17%) is roughly equivalent to 17% of the boundary layer volume being occupied by cloud, and considering the statistically high cloud cover at northern European winter locations, this is not unreasonable. More accurate calculation of the extent of cloud processing requires a convolution of the probability distribution function of cloud contact and the liquid water history during cloud contact on a case-by-case basis [*Feingold et al.*, 1998].

3.1. Sensitivity to Henry's Law Constant for NO_3

[15] We explore the sensitivity of the system to the assumed Henry's Law constant for NO_3 (g) ↔ NO_3 (aq). Values for K_{eq} in the literature range from 0.6 M atm^{-1} (at 273K; *Rudich et al.* [1996]), 1.5 M atm^{-1} (at 293K; *Thomas et al.* [1998]), 15 M atm^{-1} (*Lelieveld and Crutzen* [1991]), to as high as 2.1×10^5 M atm^{-1} (at 298K; *Pandis and Seinfeld* [1989]). The true value, as experimentally determined, is considered to be ~1 M atm^{-1} [*Rudich et al.*, 1996; *Thomas et al.*, 1998]. The value of 2.1×10^5 M atm^{-1} is considered unrealistically high; nevertheless simulations with this value are included to give an upper bound on the effect of NO_3. Results (Figure 2) show that the role of NO_3 as an oxidant is very sensitive to the assumed equilibrium constant. Table 4 shows the relative enhancement in the production of S(VI) at the end of the simulation due to the presence of NO_3 for the initial conditions in Table 3. Values are calculated as the difference in multiphase mass addition for simulations with and without NO_3, relative to the final mass of sulfate for the simulation without NO_3. The enhancement in S(VI) production ranges from about 9% to 258% and is dependent on $[H_2O_2]$, $[NO_3]$, and K_{eq} (NO_3). For given values of H_2O_2 and NO_3 the S(VI) enhancement increases with increasing K_{eq}. If one assumes that K_{eq} is on the order of 1 M atm^{-1} (our current best estimate) then the enhancement in S(VI) production is in the range of 10–30%.

3.2. Dependence on H_2O_2

[16] As shown in Table 4, the relative importance of NO_3 as an oxidant decreases with increasing H_2O_2. Figure 3 illustrates this further by showing the budget of S(VI) production for each of the cases in Figure 2, when K_{eq} = 0.6 M atm^{-1}. The oxidation rates for each case can be inferred from the slopes of the curves during cloud contact. Comparing Figures 3a and 3c, it can be seen that the dominant oxidation pathway switches from NO_3 to H_2O_2 when H_2O_2 is increased from 30 pptv to 300 pptv. A close look at the data plotted in Figure 3 shows that in an absolute sense, 20% less S(VI) is produced by NO_3 at the end of the simulation when H_2O_2 = 300 pptv. In all cases, the relative importance of H_2O_2 decreases steadily with increasing time because H_2O_2 is depleted and there is no nocturnal mechanism for replenishment. Oxidation via NO_3 maintains a fairly steady contribution to overall production and for the cases shown here, it dominates at low H_2O_2.

3.3. Sensitivity to NO_2

[17] The presence of higher fixed concentrations of NO_2 translates, in general, to higher gas-phase concentrations of NO_3 (according to (R1)), and therefore higher [NO_3 (aq)]. Note that although Figure 1 shows that $[NO_3]$ is insensitive to $[NO_2]$, this is only true in a buffered situation. In the presence of cloud droplets, N_2O_5 is rapidly removed, and $[NO_3]$ is sensitive to $[NO_2]$. Therefore, an increase in NO_2 tends to result in higher S(VI) production, and a larger contribution by NO_3 (Table 4). An exception to this occurs at low K_{eq} (= 0.6 M atm^{-1}) for H_2O_2 equal to either 30 pptv or 300 pptv. This will be explored further in section 4.1.

Table 3. Initial Gas-Phase Mixing Ratios Used as Input to the Multiphase Model[a]

	SO_2	O_3	H_2O_2	NH_3	HNO_3	CO_2	NO_3	N_2O_5
NO_2 = 30	1000	40 ppbv	30 or 300	100	1000	360 ppmv	5	1.5
NO_2 = 300	1000	40 ppbv	30 or 300	100	1000	360 ppmv	5	20

[a] Mixing ratios are given in pptv, unless otherwise stated. Values of NO_2, NO_3, and N_2O_5 are derived from the gas phase model. H_2O_2 mixing ratios are set at either 30 pptv or 300 pptv and have no bearing on NO_2, NO_3, and N_2O_5 mixing ratios.

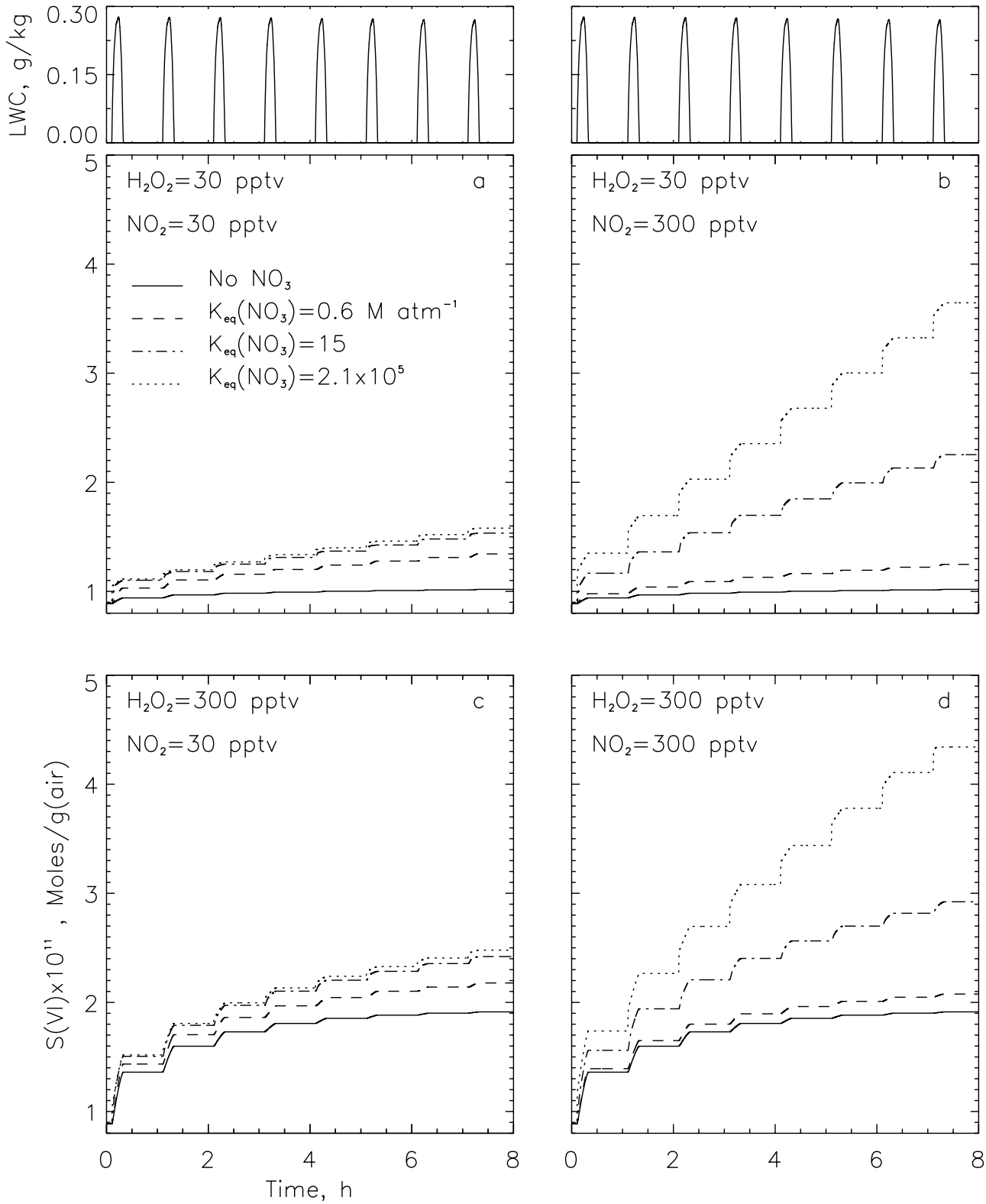

Figure 2. Upper panel: time history of parcel contact with cloud water. Lower panel: S(VI) production for an 8 h nighttime simulation for various values of K_{eq} (NO_3) in M atm^{-1} (a) initial H_2O_2 = 30 pptv, fixed NO_2 = 30 pptv; (b) initial H_2O_2 = 30 pptv, fixed NO_2 = 300 pptv; (c) initial H_2O_2 = 300 pptv, fixed NO_2 = 30 pptv; (d) initial H_2O_2 =300 pptv, fixed NO_2 = 300 pptv.

Sensitivity to the assumption of a fixed concentration of NO_2 will be examined in section 4.2.2.

4. Discussion

[18] The trends associated with S(VI) production and its dependence on K_{eq}, H_2O_2, and NO_2 are for the most part expected. With increasing solubility of NO_3, a larger proportion of the total sulfate oxidation occurs through NO_3; increasing the concentration of NO_2 allows for higher concentrations of NO_3 (g), and therefore higher concentrations of aqueous NO_3 (except when K_{eq} is low). And finally, the relative importance of NO_3 as an oxidant depends strongly on the availability of other oxidants such as H_2O_2 and O_3. In the current example, oxidation via O_3 is significantly lower than that due to H_2O_2 and NO_3 because the *p*H is less than 4. H_2O_2 is the dominant contributor to oxidation when H_2O_2 = 300 pptv, but its importance decreases with time because H_2O_2 has no major sources during the night.

4.1. Why More Sulfate is Produced by NO_3 at Lower NO_2 When k_{eq} = 0.6 m atm^{-1}

[19] Figure 3 and Table 4 show that when K_{eq} (NO_3) = 0.6 M atm^{-1} and NO_2 is increased from 30 pptv to 300 pptv, there is a decrease in the NO_3 enhancement of sulfate production, whereas the reverse is true when K_{eq} is higher. Higher [NO_2] causes faster production of NO_3 (g) via reaction (R1). The impact of higher [NO_2] on [NO_3 (g)], [NO_3 (aq)], and S(VI) production depends on the competition between the two loss processes for NO_3 (g) in the presence of cloud drops: uptake or conversion to N_2O_5 (g) (reaction (R2a)). The former channel increases [NO_3 (aq)] and S(VI) production. Any NO_3 remaining in the drop after the cloud evaporates is returned to the gas phase, so that NO_3 uptake is ultimately not a complete loss of NO_3 (g). The latter channel, conversion to N_2O_5, constitutes a rapid and permanent loss of NO_3 (g) since N_2O_5 (aq) is immediately converted to HNO_3, so that an increase in this channel decreases [NO_3 (aq)] and the NO_3 contribution to S(IV) oxidation. In the lowest K_{eq} (NO_3) case, aqueous uptake of NO_3 (g) is much slower than NO_3 (g) conversion to N_2O_5 (g), so increasing NO_2 preferentially favors NO_3 conversion to N_2O_5, an increased permanent loss of NO_3 (g), and lower [NO_3 (g)] and [NO_3 (aq)]. Conversely, when K_{eq} (NO_3) = 15 M atm^{-1}, the direct uptake of NO_3 to the drops is much faster than the loss of NO_3 through formation of N_2O_5, and increasing [NO_2] in the presence of drops now favors uptake of NO_3 (g) and increased [NO_3 (aq)]. Figures 4 and 5 highlight the differences between low and high K_{eq} (NO_3) cases and illustrate the competition between the aforementioned loss channels and their effects on [NO_3 (aq)] for high and low NO_2 conditions.

4.2. Sensitivity Studies

4.2.1. Catalytic Chain Length for NO_3 Oxidation of S(IV)

[20] All simulations thus far have assumed that the net result of the catalytic chain reaction produces 8 moles of S(VI) for every one mole of NO_3 in solution [*Rudich et al.*, 1998]. Although this result represents our current understanding of the net effect of NO_3 (aq), there is a fair degree of uncertainty associated with this value and it is therefore instructive to repeat simulations for different chain lengths.

Table 4. Enhancement in S(VI) Production Relative to the Case With No NO_3 (in %) Over the Course of 8 Hours Due to the Presence of NO_3 for Different Initial Mixing Ratios of H_2O_2 and NO_2 (in pptv) and Different Values of K_{eq}[a]

K_{eq} (NO_3), M atm^{-1}	(H_2O_2; NO_2), pptv			
	(30; 30)	(30; 300)	(300; 30)	(300; 300)
0.6	32 (28)	23 (29)	14 (13)	9 (11)
15	51	121	27	53
2.1×10^5	55	258	30	127

[a] The parenthetical values pertain to simulations where NO_2 (g) can vary during the course of a simulation according to (R1), (R2a), and (R2b) (see section 4.2.2).

If it is assumed that only 4 moles of S(VI) are produced for every mole of NO_3 in solution, our simulations show that the enhancement in sulfate production due to NO_3 can be scaled by approximately one half. Assuming K_{eq} (NO_3) = 0.6 M atm^{-1}, the percentage enhancement in S(VI) is reduced from 10–30% to 5–15% for the cases studied here. Similarly, if the chain length is longer, then increases in S(VI) production will scale upward accordingly.

4.2.2. Assumption of Fixed NO_2

[21] Simulations presented in section 3 assumed, for simplicity, that NO_2 has a fixed mixing ratio for the duration of the simulation. In reality, in the absence of local sources, NO_2 will be depleted as a result of reaction (R2a) followed by uptake of N_2O_5 on drops. A number of simulations were repeated while relaxing the assumption of constant NO_2 when solving (R1), (R2a), and (R2b). For K_{eq} (NO_3) = 0.6 M atm^{-1}, H_2O_2 = 30 pptv, and initial NO_2 = 30 pptv, the percentage increase in sulfate production is 28% rather than the 32% quoted for fixed NO_2 (Table 4). When H_2O_2 = 300 pptv and initial NO_2 = 300 pptv, the enhancement in sulfate production increases from 9% to 11%. This is because NO_2 decreases to about 90 pptv by the end of the simulation, which in accord with our discussion in section 4.1, suggests an increase in NO_3 (aq). These results are shown in parentheses in Table 4 for K_{eq} (NO_3) = 0.6 M atm^{-1}.

4.2.3. Assumption of Complete Outgassing of HNO_3

[22] In the results presented here, we did not consider permanent removal of HNO_3 as particulate inorganic nitrate. The result is a bias towards higher HNO_3 (g), which reduces *p*H and affects oxidation via the O_3 pathway. In order to test the sensitivity of the results to this assumption, a simulation was performed in which all N(V) species were assumed to be converted to particulate nitrate. Such a simulation provides an upper bound on the effect of this assumption. The simulation for H_2O_2 = 30 pptv and NO_2 = 30 pptv, for K_{eq} (NO_3) = 0.6 M atm^{-1}, shows an increase in the contribution of O_3 to total sulfate because *p*H is higher, as well as an increase in the total amount of sulfate produced. The overall impact of NO_3 on S(IV) oxidation is reduced from 32% to 15%. In reality, only part of the aqueous HNO_3 would be removed as particulate matter, and the effects on the NO_3 contribution to sulfate production would be intermediate between these two extremes.

4.3. Feedbacks of Chemistry to Aerosol and Cloud Microphysics

[23] The uptake of soluble gases and formation of S(VI) is a drop-size dependent process, primarily due to variability in the surface to volume ratio, and the change in *p*H as a

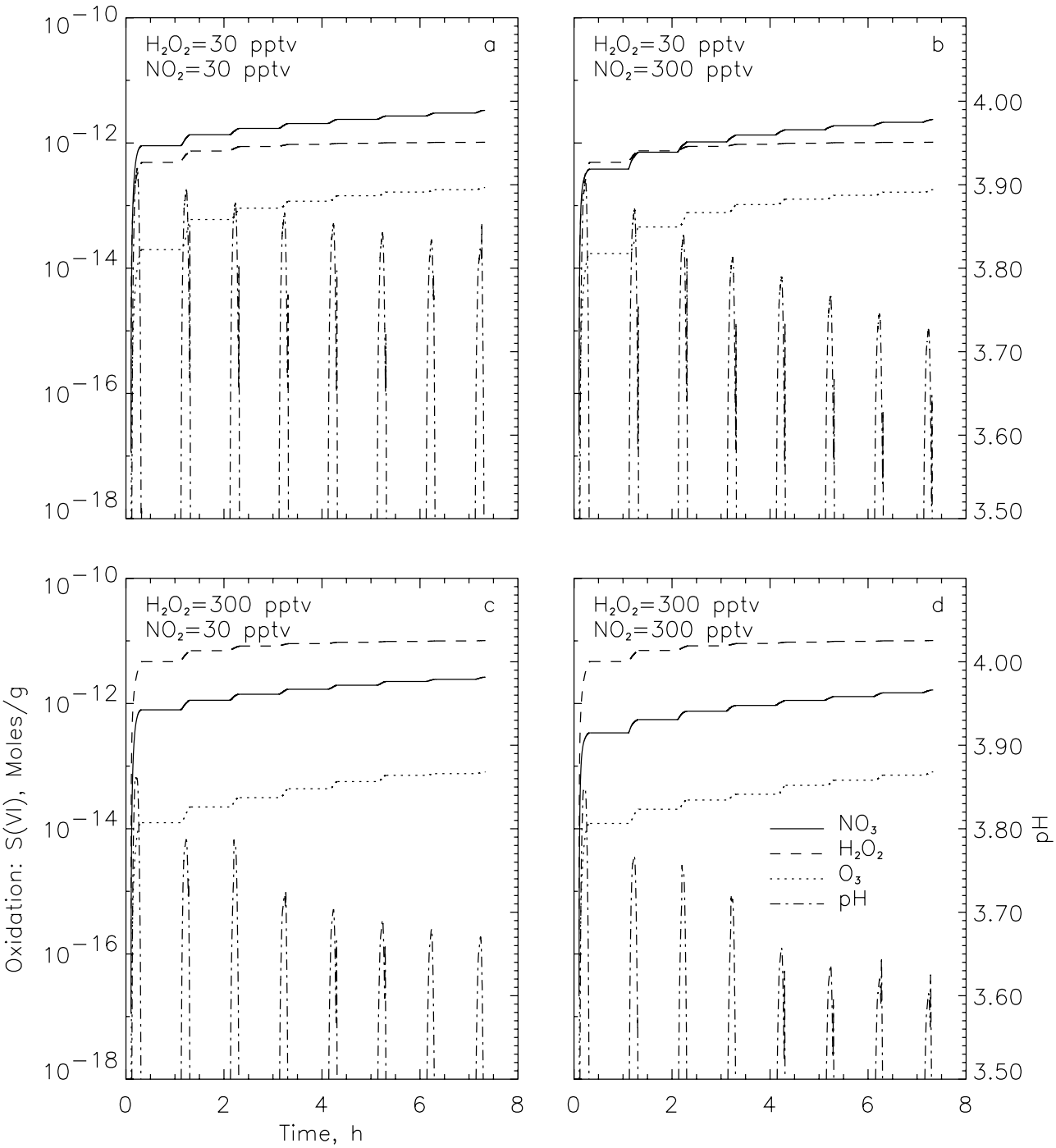

Figure 3. Budgets of S(IV) oxidation due to H_2O_2, NO_3, and O_3, and for K_{eq} = 0.6 M atm^{-1}; (a) initial H_2O_2 = 30 pptv, fixed NO_2 = 30 pptv; (b) initial H_2O_2 = 30 pptv, fixed NO_2 = 300 pptv; (c) initial H_2O_2 = 300 pptv, fixed NO_2 = 30 pptv; (d) initial H_2O_2 = 300 pptv, fixed NO_2 = 300 pptv. Oxidation rates can be inferred from the slopes of the curves during cloud contact. The pH is superimposed.

function of drop size. To explore the extent to which the results presented here are robust with respect to the representation of cloud microphysics, the simulations have been repeated with a version of the model that resolves only one size category of aerosol particles. Some minor modifications were made to the model to constrain the total drop concentration to be similar to that calculated by the 10-size category model (~270 cm^{-3}). First, when considering the results in the absence of NO_3 we find that less S(VI) mass is added to the system over an 8 h period: for 10 size categories, the amount is 1.30 Moles g^{-1} vs. 1.15 Moles g^{-1} for one size category (a decrease of 11%). When considering the simulations with NO_3, and for various K_{eq} (NO_3), the results for one size category are quantitatively somewhat different from those for 10 size categories (Table 5) although the trends are the same. Most notably, the reduction in S(VI) enhancement due to NO_3 when K_{eq} (NO_3) = 0.6 M atm^{-1} and NO_2 is increased from 30 pptv to 300 pptv (see section 4.1) is still

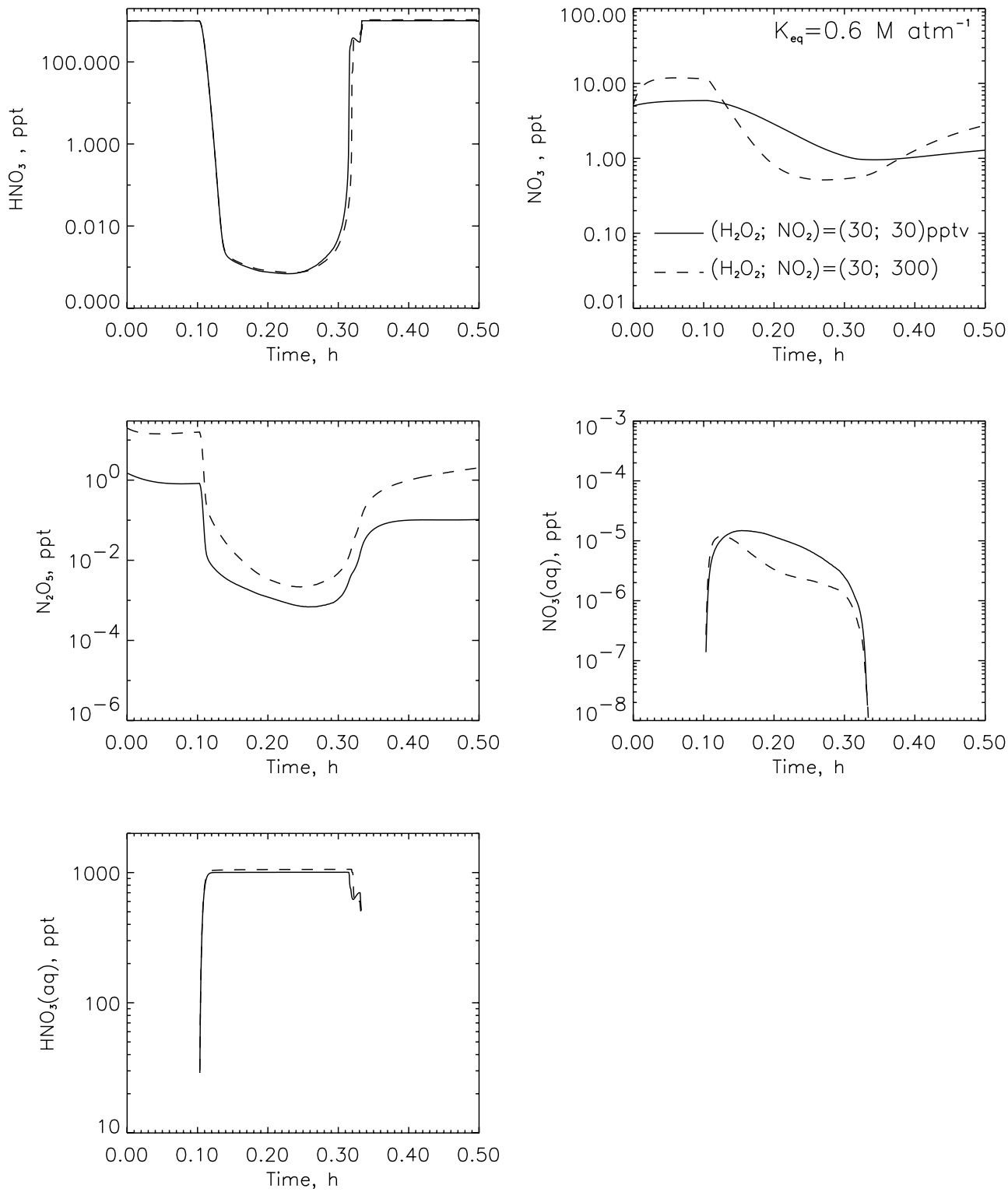

Figure 4. Comparison of various gas and aqueous fields for K_{eq} (NO_3) = 0.6 M atm^{-1}; Solid line: initial H_2O_2 = 30 pptv, fixed NO_2 = 30 pptv, and dashed line: initial H_2O_2 = 30 pptv, fixed NO_2 = 300 pptv.

apparent, and confirms our contention that this result is not due to microphysical feedbacks.

[24] These results highlight the fact that much information can be obtained using a more simple representation of cloud microphysics but that, as shown by previous studies [e.g., *Gurciullo and Pandis*, 1997], the size distribution can under some circumstances underestimate the extent of sulfate production.

4.4. Other Factors Affecting the Role of NO_3

[25] We have modeled the variation of sulfate formation with time and the enhancement of sulfate formation due to

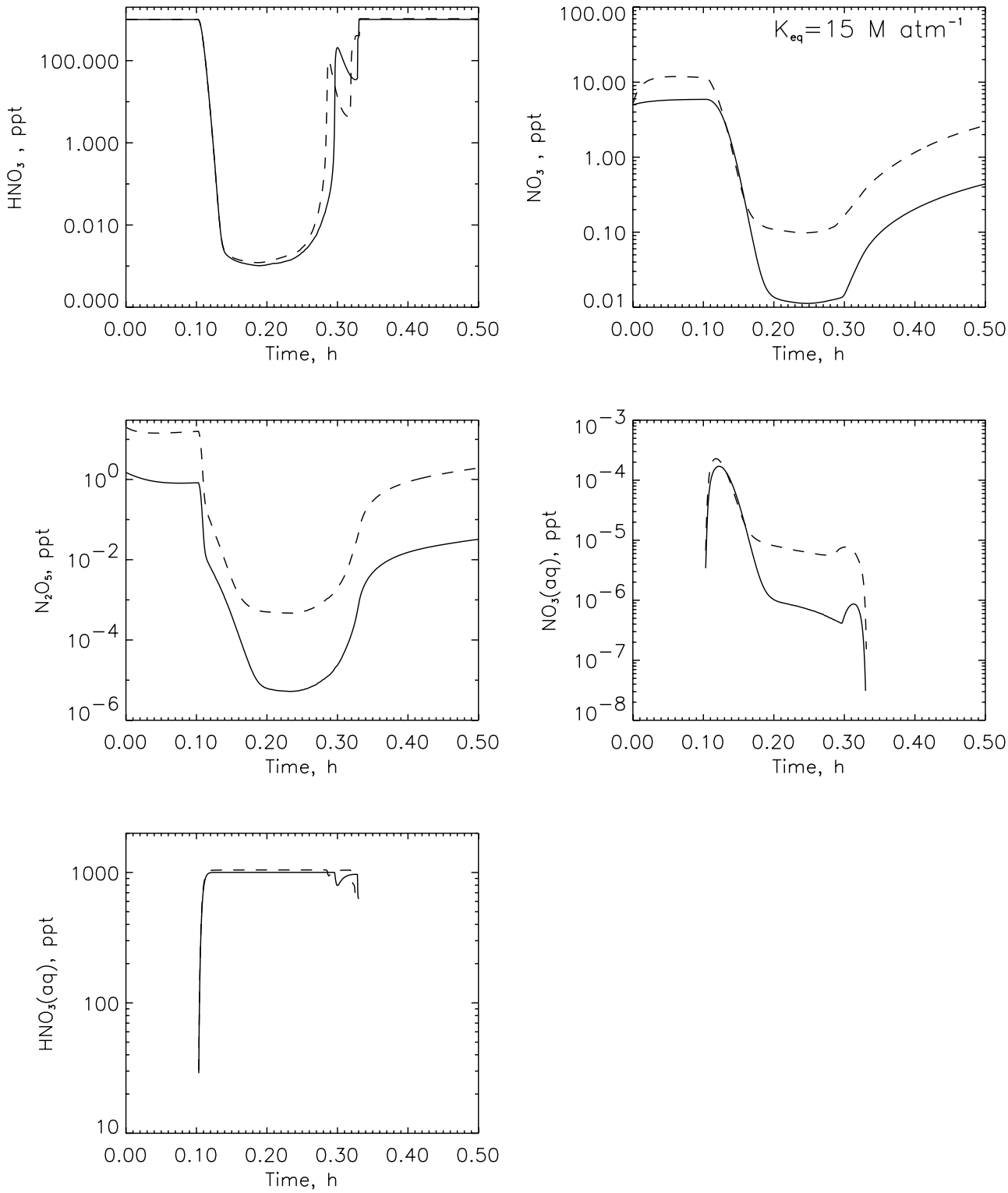

Figure 5. As in Figure 4 but for K_{eq} (NO_3) =15 M atm^{-1}.

the reactions of NO_3 in liquid droplets for those conditions where only H_2O_2 and O_3 can oxidize SO_2. As can be seen, the enhancement due to NO_3 may be important. There are other factors that would modify the role of NO_3 in sulfate formation and these are now discussed qualitatively.

[26] This study has only considered non-precipitating clouds. However, it is possible, and even likely, that precipitation will selectively remove the soluble H_2O_2. Under these conditions, the role of NO_3 in sulfate production will be enhanced. Because NO_2, SO_2, and O_3 are not very water soluble, they will remain in the gas phase so that they can then be subjected to further multiphase processing.

[27] While SO_2 and NO_2 are both emitted by certain fossil-fuel combustion sources, NO_x may also be emitted by

Table 5. As in Table 4, but for 1 Size Category of Aerosol/Drops

K_{eq} (NO_3), M atm^{-1}	(H_2O_2; NO_2), pptv			
	(30; 30)	(30; 300)	(300; 30)	(300; 300)
0.6	48	31	15	8
15	84	191	33	64
2.1×10^5	91	421	37	158

a variety of sources without a corresponding emission of SO_2. Therefore, as an air mass moves away from a source of both SO_2 and NO_x, more NO_x can mix in and modify the role of NO_3 in converting SO_2 to sulfate. We express the caveat that, as discussed in section 4.1, higher NO_2 does not always translate to higher aqueous NO_3 if the solubility of NO_3 is low.

[28] Finally, the initial gas phase abundance of H_2O_2 in our calculations did not depend on the concentration of NO_2. However, in cloud-free air masses with larger NO_x abundances, H_2O_2 will be relatively suppressed because the ratio of HO_2 to OH will be lowered in the presence of higher NO. Therefore, in NO_x-rich conditions, the relative contribution of NO_3 to sulfate production will tend to be larger because of lower [H_2O_2] (e.g., Figure 3). (The loss of NO_3 to N_2O_5 (reaction (R2a)) will tend to reduce NO_3, but higher NO_2 is still likely to result in higher NO_3.) With respect to the relative roles of NO_3 and H_2O_2, it should also be mentioned that various multiphase reactions may result in a net production of H_2O_2 by clouds however this occurs during the daytime, and under high NO_x/low H_2O_2 conditions [*Kim et al.*, 2002].

[29] These possible impacts are for the most part likely to increase the calculated role of NO_3 in converting SO_2 to sulfate under conditions where there is a deficit in the calculated sulfate production. A more comprehensive model should better clarify the role of NO_3 in sulfate production.

5. Conclusions

[30] Under conditions of low light (and therefore low OH and H_2O_2), NO_3 may play a measurable role as an oxidant of S(IV), provided there is a source of gas phase NO_2. At nighttime, H_2O_2 is depleted by clouds over the course of a few hours and is not replenished by gas phase chemistry. O_3 is not effective as an oxidant in the cases examined here because of the low *p*H. On the other hand, NO_3 persists because it is produced in the gas phase by (R1) and (R2b). The relative importance of NO_3 in the high-latitude northern winter therefore increases with increasing duration of cloud contact, and increasing time after sunset.

[31] As shown in this paper, the relative importance of NO_3 oxidation of S(IV) is also dependent on a number of other factors.

1. The first factor is Henry's Law constant (K_{eq}) for NO_3 (g) $\leftrightarrow$ NO_3 (aq). For a value of 0.6 M atm^{-1}, NO_3 is expected to play a measurable role (10–30%) for the conditions simulated here. If K_{eq} (NO_3) is 15 M atm^{-1}, the enhancement in S(VI) production ranges from 25–120%. Laboratory measurement of the Henry's Law constant for NO_3 over a range of atmospheric temperatures is therefore important.

2. The second factor is catalytic chain length for NO_3 oxidation of S(IV). The base results presented suggest a 10–30% enhancement in S(VI) production assuming a catalytic chain length of 8. Sensitivity tests show that the role of NO_3 scales linearly with the chain length. Further work is needed to reduce uncertainty in this chain length to quantify the role of NO_3 to greater accuracy.

3. The third factor is the relative importance of NO_3 increases with decreasing H_2O_2, and increasing NO_2. The exception to the NO_2 sensitivity is at low K_{eq} (0.6 M atm^{-1}) where permanent loss of N_2O_5 to drops (which is much stronger when NO_2 is high) dominates NO_3 uptake and results in removal of gas phase NO_3, less NO_3 (aq), and less conversion via the NO_3 pathway. As K_{eq} increases, more NO_3 is partitioned into the aqueous phase where it can be directly applied to conversion of S(IV) to S(VI).

[32] Models that simulate global sulfate production but neglect the role of NO_3 underpredict sulfate formation in the wintertime northern high latitudes compared with observations. The simple model used here to address the relative importance of NO_3 and H_2O_2 in sulfate production suggests a role for NO_3 under these conditions. Other factors may be at play, such as boundary layer cloudiness, wet deposition, heterogeneous reactions on aerosols [*Kasibhatla et al.*, 1997], etc., and therefore one cannot draw firm conclusions about the source of the discrepancy. However, inclusion of NO_3 induced sulfate production in global models appears to be warranted.

[33] To clarify the role of NO_3, a more comprehensive model that includes coupled gas and multiphase components, as well as dynamically evolving, precipitating clouds should be applied. Concurrently, given the sensitivity of the results to NO_3, field measurements of [NO_3] are necessary to establish the importance of oxidation via NO_3, as well as for a consistency check on the model calculations.

[34] **Acknowledgments.** The microphysical cloud-chemistry model used in this study is the outgrowth of a model developed as part of a collaborative research effort with Sonia M. Kreidenweis, Colorado State University. A.R.R. was partially funded by NOAA's Climate and Global Change Research Program.

References

Atkinson, R., *Gas-Phase Tropospheric Chemistry of Organic Compounds*, *J. Phys. Chem. Ref. Data Monogr. 2*, Am. Chem. Soc., New York, 1994.

Barth, M. C., P. J. Rasch, J. T. Kiehl, C. M. Benkovitz, and S. E. Schwartz, Sulfur chemistry in the National Center for Atmospheric Research Community Climate Model: Description, evaluation, features, and sensitivity to aqueous chemistry, *J. Geophys. Res.*, *105*, 1387–1415, 2000.

Brown, P. N., G. D. Byrne, and A. C. Hindmarsh, VODE: A variable coefficient ODE solver, *SIAM J. Sci. Stat. Comput.*, *10*, 1038–1051, 1989.

DeMore, W. B., S. P. Sander, D. M. Golden, R. F. Hampson, M. J. Kurylo, C. J. Howard, A. R. Ravishankara, C. E. Kolb, and M. J. Molina, Chemical kinetics and photochemical data for use in stratospheric modeling: Evaluation number 12, *JPL Publ., 97-4*, 1997.

Feingold, G., S. M. Kreidenweis, and Y. Zhang, Stratocumulus processing of gases and cloud condensation nuclei, 1, Trajectory ensemble model, *J. Geophys. Res.*, *103*, 19,527–19,542, 1998.

Frost, G. J., et al., Photochemical ozone production in the rural southeastern United States during the 1990 Rural Oxidants in the Southern Environment (ROSE) program, *J. Geophys. Res.*, *103*, 22,491–22,508, 1998.

Fuchs, N. A., and A. G. Sutugin, High-dispersed aerosols, *Int. Rev. Aerosol Phys. Chem.*, *2*, 1–60, 1971.

Gardner, J. A., L. R. Watson, Y. G. Adewuyi, P. Davidovits, M. S. Zahniser, D. R. Worsnop, and C. E. Kolb, Measurement of the mass accommodation coefficient of SO_2 (g) on water droplets, *J. Geophys. Res.*, *92*, 10,887–10,895, 1987.

Gurciullo, C. S., and S. N. Pandis, Effect of composition variations in cloud droplet populations on aqueous-phase chemistry, *J. Geophys. Res.*, *102*, 9375–9385, 1997.

Hoffmann, M. R., and J. G. Calvert, Chemical transformation modules for

Eulerian acid deposition models, vol. 2, The aqueous-phase chemistry, *EPA/600/3-85/036*, U.S. Environ. Prot. Agency, Research Triangle Park, N. C., 1985.

Kasibhatla, P., W. L. Chameides, and J. St. John, A three dimensional global model investigation of seasonal variation in the atmospheric burden of anthropogenic sulfate aerosols, *J. Geophys. Res.*, *102*, 3737–3760, 1997.

Kim, C.-H., S. M. Kreidenweis, G. Feingold, G. J. Frost, and M. K. Trainer, Modeling cloud effects on hydrogen peroxide and methylhydroperoxide in the marine atmosphere, *J. Geophys. Res.*, *107*(D2), 4018, doi:10.1029/2000JD000285, 2002.

Lelieveld, J., and P. J. Crutzen, The role of clouds in tropospheric chemistry, *J. Atmos. Chem.*, *12*, 229–267, 1991.

Mozurkewich, M., Mechanism for the release of halogens from sea salt particles by free radical reactions, *J. Geophys. Res.*, *100*, 14,199–14,207, 1995.

Müller, F., Estimation of the effect of operator splitting on detailed aerosol growth including multiphase chemistry, paper presented at 13th International Conference on Clouds and Precipitation, World Meteorol. Organ., Reno, Nev., 2000.

Pandis, S., and J. H. Seinfeld, Sensitivity analysis of a chemical mechanism for aqueous-phase atmospheric chemistry, *J. Geophys. Res.*, *94*, 1105–1126, 1989.

Rudich, Y., R. K. Talukdar, A. R. Ravishankara, and R. W. Fox, Reactive uptake of NO_3 on pure water and ionic solutions, *J. Geophys. Res.*, *101*, 21,023–21,031, 1996.

Rudich, Y., R. K. Talukdar, and A. R. Ravishankara, Multiphase chemistry of NO_3 in the remote troposphere, *J. Geophys. Res.*, *103*, 16,133–16,143, 1998.

Sander, R., J. Lelieveld, and P. J. Crutzen, Model study of the nighttime nitrogen and sulfur chemistry in size resolved droplets of an orographic cloud, *J. Atmos. Chem.*, *20*, 16–89, 1995.

Schwartz, S. E., Mass-transport considerations pertinent to aqueous-phase reactions of gases in liquid-water clouds, in *Chemistry of Multiphase Atmospheric Systems*, edited by W. Jaeschke, pp. 415–471, Springer-Verlag, New York, 1986.

Stevens, B., G. Feingold, W. R. Cotton, and R. L. Walko, On elements of the microphysical structure of numerically simulated stratocumulus, *J. Atmos. Sci.*, *53*, 980–1006, 1996.

Tang, I. N., and J. H. Lee, Accommodation coefficients of ozone and SO_2: Implications on SO_2 oxidation in cloud water, in *The Chemistry of Acid Rain, Sources and Atmospheric Processes*, edited by R. W. Johnson et al., Am. Chem. Soc., Washington D. C., 1987.

Thomas, K., A. Volz-Thomas, D. Mihelcic, H. G. J. Smit, and D. Kley, On the exchange of NO_3 radicals with aqueous solutions: Solubility and sticking coefficient, *J. Atmos. Chem.*, *29*, 17–43, 1998.

Warren, S. G., C. J. Hahn, J. London, R. M. Chervine, and R. L. Jenne, Global distribution of total cloud cover and cloud type amounts over land, *NCAR Tech. Note*, *NCAR/TN-273+STR*, 29 pp., 1986a.

Warren, S. G., C. J. Hahn, J. London, R. M. Chervine, and R. L. Jenne, Global distribution of total cloud cover and cloud type amounts over ocean, *NCAR Tech. Note*, *NCAR/TN-317+STR*, 42 pp., 1986b.

Zhang, Y., S. M. Kreidenweis, and G. Feingold, Stratocumulus processing of gases and cloud condensation nuclei, 2, Chemistry sensitivity analysis, *J. Geophys. Res.*, *104*, 16,601–16,080, 1999.

G. Feingold, NOAA Environmental Technology Laboratory, 325 Broadway, Boulder, CO 80305, USA. (graham.feingold@noaa.gov)

G. J. Frost and A. R. Ravishankara, NOAA Aeronomy Laboratory, Mail Stop R/E/AL4, 325 Broadway, Boulder, CO 80305, USA. (gfrost@al.noaa.gov; ravi@al.noaa.gov)